

pubs.acs.org/NanoLett Letter

Operando Investigation of Locally Enhanced Electric Field Treatment (LEEFT) Harnessing Lightning-Rod Effect for Rapid Bacteria Inactivation

Ting Wang, Devin K. Brown, and Xing Xie*



Cite This: https://doi.org/10.1021/acs.nanolett.1c02240



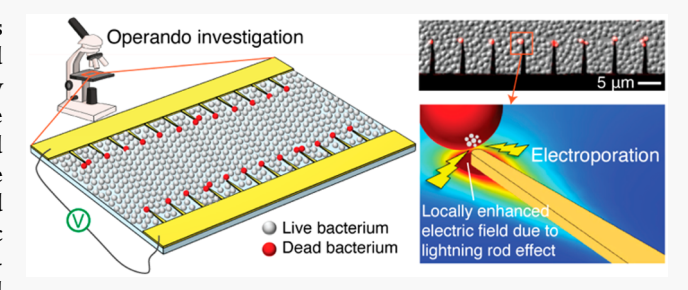
ACCESS

III Metrics & More

Article Recommendations

Supporting Information

ABSTRACT: The growth of undesired bacteria causes numerous problems. Here, we show that locally enhanced electric field treatment (LEEFT) can cause rapid bacteria inactivation by electroporation. The bacteria inactivation is studied *in situ* at the single-cell level on a lab-on-a-chip that has nanowedge-decorated electrodes. Rapid bacteria inactivation occurs at the nanowedge tips where the electric field is enhanced due to the lightning-rod effect. Electroporation induced by the locally enhanced electric field is the predominant mechanism. The antimicrobial performance depends on the strength of the enhanced electric field instead



of the applied voltage, and no generation of reactive oxygen species (ROS) is detected when >90% bacteria inactivation is achieved. Quick membrane pore closure under lower voltages confirms that electroporation is induced in LEEFT. This work is the first-time visualization and mechanism elucidation of LEEFT for bacteria inactivation at the single-cell level, and the findings will provide strong support for its future applications.

KEYWORDS: Locally enhanced electric field treatment, Lightning-rod effect, Electroporation, Antimicrobial, Nanostructures, Operando investigation

B acteria are indispensable for both ecological systems and human bodies, but the growth of undesired bacteria can cause serious problems. Seeking approaches for bacteria inactivation is an everlasting effort. Most of our current practices for bacteria inactivation highly rely on the uses of chemicals, such as antibiotics for infection treatment, chlorine for water disinfection, and chemical antifouling agents. They have been effectively inactivating bacteria, but caused new problems: overuse of antibiotics has already raised the concern of antibiotic resistance; 1 chlorination generates disinfection byproducts (DBPs) that can be carcinogenic; 2 and antifouling agents may be harmful to human health or the environment.

Effective physical processes, such as thermo/ultraviolet radiation,^{3,4} acoustic vibration,^{5,6} microwave,⁷ and electric field treatment (EFT),⁸ can be superior alternatives to chemical approaches for bacteria inactivation, although many of them suffer from high capital cost or energy consumption. Among these processes, EFT is increasingly finding applications in food preservation and water disinfection.^{9–12} EFT aims to inactivate bacteria by electroporation: when a cell is exposed to a strong electric field, an induced transmembrane voltage (TMV) will cause pore formation on the lipid bilayer membrane; ^{13–15} when this external electric field is strong enough, the membrane damage, that is, the pores, will become lethal to the bacterial cells.¹⁰ The lethal electroporation threshold was found to be between 10–35 kV/cm. ¹⁶ Typically,

in order to achieve the strong electric field, EFT processes require high applied voltages (e.g., \sim 23 kV to achieve 35 kV/cm on a 0.65 cm gap), ¹⁷ which lead to safety issues, side reactions, and high energy consumption.

A strategy to realize the high electric field strength with lower voltages is to decorate the electrodes with sharp objects, such as nanowires or nanowedges, for locally enhanced electric field treatment (LEEFT). Attributed to the lightning-rod effect, the electric field near the tips could be largely enhanced depending on the aspect ratio of the electrode decorations. As a result, even with relatively low applied voltages, the locally enhanced electric field can still build up the transmembrane voltage that is sufficient to cause irreversible electroporation and bacteria inactivation. Although this concept has been claimed as the predominant mechanism for bench-scale EFT water disinfection devices equipped with nanowire-modified electrodes, 19–28 direct demonstration of lightning-rod effect for bacteria inactivation, especially at the single-cell level, is not yet

Received: June 8, 2021
Revised: October 31, 2021



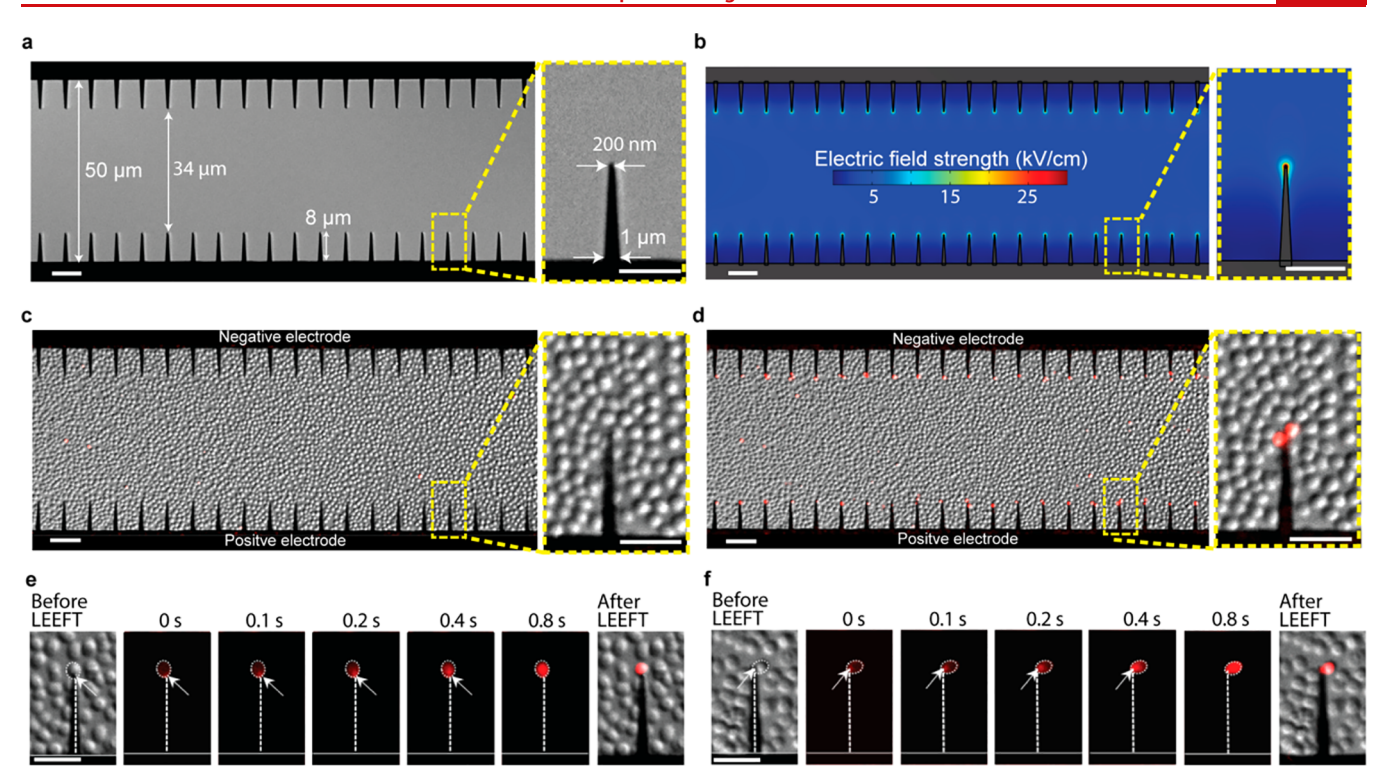


Figure 1. Bacteria damage in LEEFT. (a) Microscopy images of the lab-on-a-chip. (b) The nanoenhanced electric field at the nanowedge tips under 18 V applied voltage. (c, d) Microscopy images of the immobilized bacteria cells before (c) and after (d) treatment. Scale bars are 10 μ m in normal images and 5 μ m in the zoom-in images. (e, f) PI fluorescence onset indicating pore formation position of a cell at nanowedge tip on negative electrode (e) and positive electrode (f). The arrows indicate the position of the cell membrane adjacent to the nanowedge tip, which is also the onset position of PI fluorescence. The scale bars are 5 μ m.

done. Here, we conduct LEEFT on a lab-on-a-chip device that has nanowedge-modified electrodes and investigate the bacteria inactivation process *in situ*. Results show that the bacteria located at the tips of nanowedges on both positive and negative electrodes are rapidly inactivated in LEEFT. Electroporation induced by the locally enhanced electric field attributed to the lightning-rod effect is the predominant mechanism for this bacteria inactivation. It is the first-time process visualization and mechanism illustration of LEEFT at the single-cell level. The findings of this work will provide strong supports for the future applications of LEEFT.

Lab-on-a-chip has been intensively used for operando investigation of microbiology-related processes. 13,29,30 We developed a lab-on-chip device with gold nanowedges fabricated on both positive and negative electrodes (Figure 1a and Figure S1) to enable the operando investigation. The gap between the two electrodes is 50 μ m. The length and thickness of the nanowedge are 8 μ m and 200 nm, respectively. The width of the nanowedge tip is 200 nm, and it gradually increases to 1 μ m to allow a steadier connection to the bulk electrode. This is the default chip design in this work unless otherwise stated. When a voltage is applied to the two electrodes, the electric field near the nanowedge tips will be enhanced due to the lightning-rod effect, which is simulated using COMSOL Multiphysics (Figure 1b).

The chip was precoated with positively charged poly-L-lysine, and the model bacteria *Staphylococcus epidermidis* (*S. epidermidis*) were uniformly distributed and firmly immobilized on the chip since they are negatively charged (Figure 1c). Liveand-dead cell distinguishing stain propidium iodide (PI) was added in the deionized water (DI water) medium before

treatment (see experimental setup in Figure S2a). After 500 000 electrical pulses at 18 V with 2 μ s pulse width and 100 μ s period are applied (denoted as 18 V/2 μ s/100 μ s/500 000 pulses, see the waveform in Figure S3), the bacteria at the tips of nanowedges on both positive and negative electrodes show red fluorescence of the PI stain, indicating cell membrane damage, while other bacteria are still intact (Figure 1d). The zoom-in image clearly shows that only the cells located very close to the nanowedge tips are damaged, which is consistent with the electric field enhancement pattern (Figure 1b). By comparison, for the electrodes that have no nanowedge modification but a smaller gap of 34 μ m, hardly any cells are affected (Figure S4), suggesting that this electrical treatment is not sufficient to kill bacteria in bulk or on the electrode edge.

The bacteria damage process was observed in real-time. The onset position of PI fluorescence indicates that the cell membrane damage takes place at the position adjacent to the nanowedge tip, where the nanoenhanced electric field has the highest strength. The circled bacteria cells at the nanowedge tips on the negative electrode (Figure 1e) and positive electrode (Figure 1f) do not show fluorescence before the treatment (0 s). The arrows indicate the location where the cell membrane is adjacent to the nanowedge tip. After the treatment starts, the red fluorescence of PI stain first originates from the adjacent point indicated by the arrows (shown in 0.1, 0.2, and 0.4 s), suggesting that the part of the cell membrane subjected to the strongest electric field will be perforated first.

The bacteria damage occurs rapidly in LEEFT, which can be seen from the video Movie S1. To figure out how fast it is, different effective treatment time (i.e., the total time that the

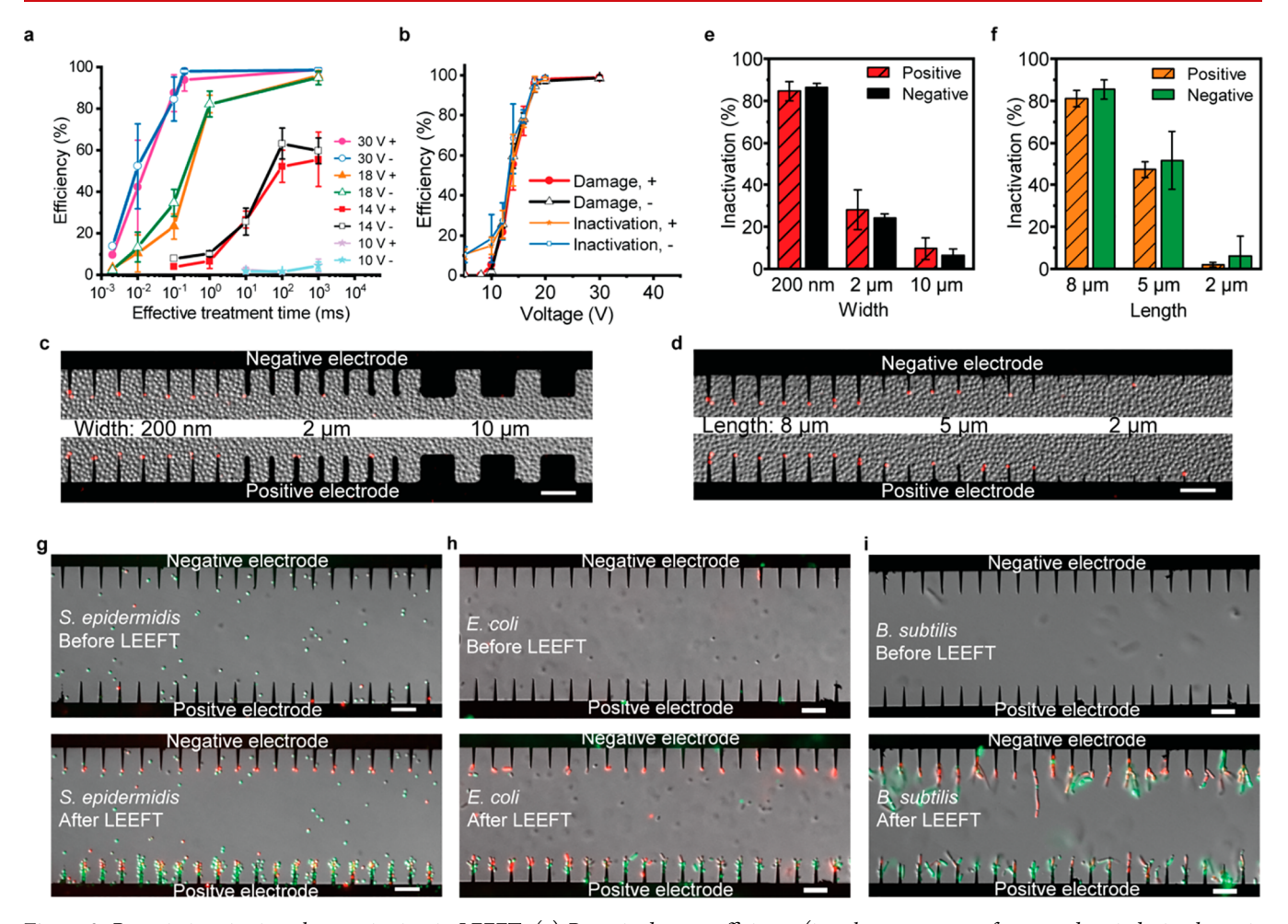


Figure 2. Bacteria inactivation characterization in LEEFT. (a) Bacteria damage efficiency (i.e., the percentage of nanowedges inducing bacteria damage) at different effective treatment time. Positive and negative electrodes are denoted as + and -, respectively. (b) Bacteria damage and inactivation efficiency versus the applied voltage with 1 s effective treatment time. (c-f) Bacteria inactivation with wedges of different width (c, e) and different length (d, f). (g-i) Microscopy images of different kinds of free-moving bacteria in the medium before (top) and after (bottom) LEEFT. (g) S. epidermidis. (h) E. coli. (i) B. subtilis. The scale bars are 10 μ m.

applied voltage is not zero, equals to pulse width X pulse number) was tested by applying different numbers of 2 μ s/100 μs pulses. Under 30 and 18 V applied voltage, 0.1 and 1 ms effective treatment time is long enough to achieve >80% bacteria damage (represented by the percentage of nanowedges inducing bacteria damage at their tips), respectively, indicating that bacteria damage in LEEFT is very rapid (Figure 2a). Under relatively lower applied voltages (14 and 10 V), bacteria damage stays at low percentage even with 1 s effective treatment time, suggesting that the limiting factor of the lower bacteria damage is the applied voltage rather than treatment time (Figure 2a). Therefore, the bacteria damage efficiency at different applied voltages with 1 s effective treatment time was tested. In case the cell damage was reversible, we conducted parallel experiments but stained the cells 2 hours after treatment with PI. Since reversible membrane damages should already recover after 2 hours, the cells stained with PI are considered inactivated.¹⁴ There is no significant difference between the efficiency of cell damage and inactivation, except that cell inactivation is slightly higher at low voltages (Figure 2b), which is due to random cell inactivation in all cells after 2 hours. The efficiency shows a positive correlation with the applied voltage (Figure 2b). The cell damage starts at a low voltage of 10 V, and 20 V is already high enough to achieve

bacteria inactivation for almost all nanowedges. No significant difference is observed between the positive and negative electrodes. This result indicates that with 1 s effective treatment time, most cell damage is irreversible, leading to cell inactivation. This is further confirmed by the phenomenon that the damaged bacteria lost cell integrity and decayed after being stored in nutrient broth at 35 °C for 6 h (Figure S5). Therefore, when 1 s effective time (500 000 pulses) is used, we consider the cell inactivation efficiency is approximately the same with cell damage.

The high aspect ratio of the nanowedges is important to LEEFT, indicated by the control experiments with different chip designs (Figure 2c-f). After the treatment of 18 V/2 μ s/100 μ s/500 000 pulses, the nanowedges with 200 nm width (Figure 2c,e) and 8 μ m length (Figure 2d,f) show a much higher efficiency of bacteria inactivation than other wider or shorter wedges. LEEFT also works for free-moving bacteria cells suspended in the medium. SYTO 9 and PI-stained S. epidermidis are suspended in DI water before the treatment (Figure 2g top; see the experimental setup in Figure S2b). During the treatment (18 V/2 μ s/100 μ s/500 000 pulses), bacteria cells are attracted toward the nanowedges on both positive and negative electrodes, especially to the tips. Subsequently, those near the tips become inactivated, indicated

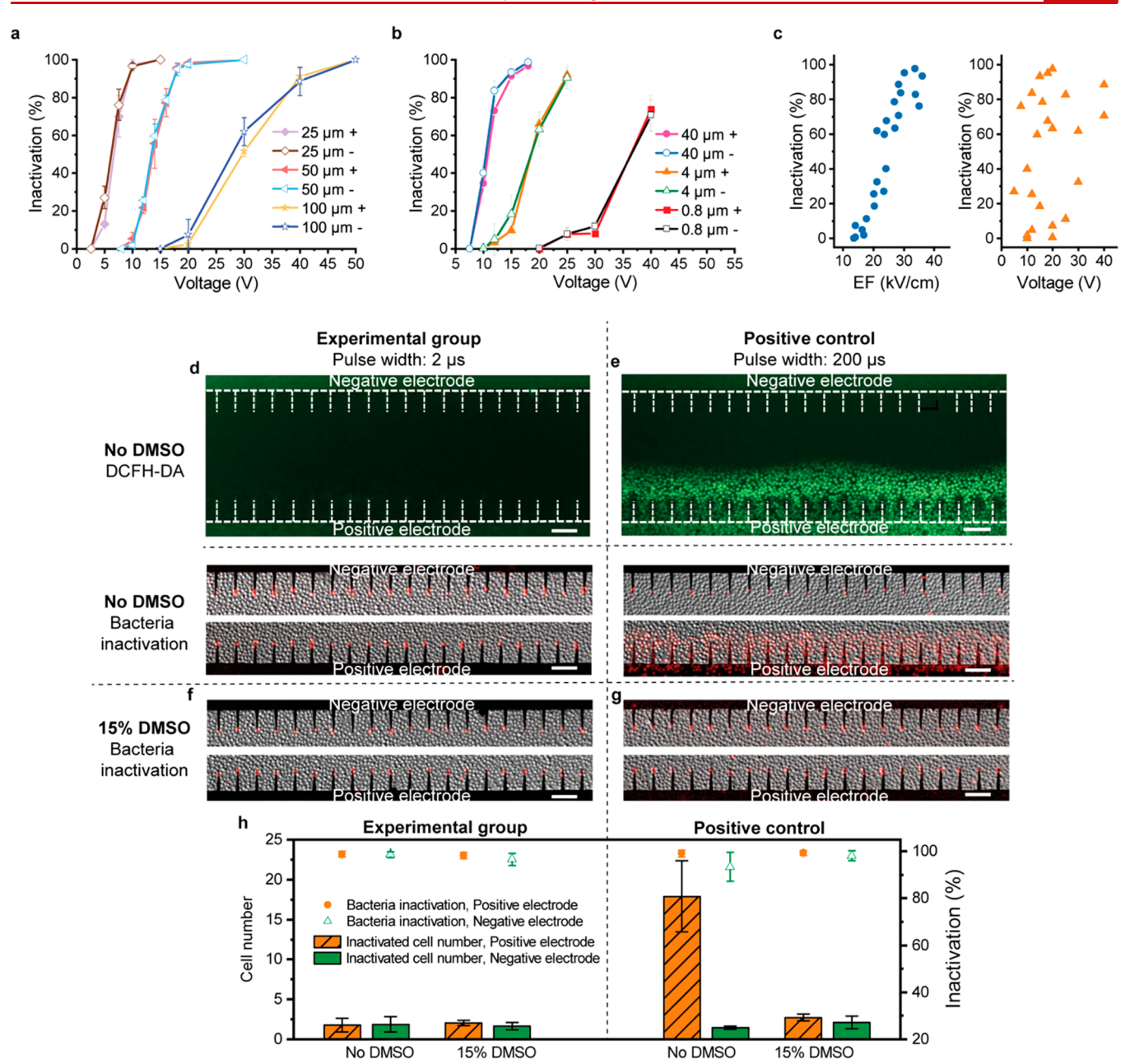


Figure 3. Antibacterial mechanism study. (a) Bacteria inactivation on chips of different gaps between positive and negative electrodes. (b) Bacteria inactivation on chips of different intervals between nanowedges. (c) Relationship between the bacteria inactivation and the electric field strength (EF) at the tip of the nanowedge (0.1 μ m away from the nanowedge tip) (left), and the applied voltages (right). (d) Fluorescence of DCFH-DA-stained cells (top), and bacteria inactivation with no DMSO (bottom) in the experimental group. (e) Fluorescence of DCFH-DA-stained cells (top), and bacteria inactivation with no DMSO (bottom) in the positive control group. Green fluorescence indicates ROS generation. (f, g) Bacteria inactivation with 15% DMSO in (f) experimental group and (g) positive control. (h) Bacteria inactivation percentage and the average inactivated cell number at each nanowedge tip. The scale bars are 10 μ m.

by switching from the green fluorescence of SYTO 9 to the red fluorescence of PI (Movie S2, Figure 2g bottom). As the bacteria cells are negatively charged in DI water, most of them accumulate at the positive electrode because of the electrophoretic force. Some cells are attracted to the nanowedge tips on the negative electrode, which is probably due to the strong dielectrophoretic force induced by the strong and nonuniform electric field near the tips.^{27,31} Two other strains of bacteria, *Bacillus subtilis* (*B. subtilis*, Gram +) and *Escherichia coli* (*E. coli*, Gram –), are also tested, which show similar transport and inactivation phenomena with *S. epidermidis* (Figure 2h,i,

Movies S3 and S4), suggesting that LEEFT could be a wide spectrum bacteria inactivation method.

In LEEFT, only the bacteria located near nanowedge tips are inactivated, while bacteria in bulk are not affected. This pattern is consistent with the electric field enhancement due to the lightning-rod effect, suggesting that irreversible electroporation induced by the enhanced electric field is the most possible mechanism for bacteria inactivation. Here, we investigated on the mechanism and discuss the collected evidence.

First, we found that the bacteria inactivation depends on the strength of the nanoenhanced electric field rather than the applied voltage. Chips of different positive/negative electrode

Nano Letters pubs.acs.org/NanoLett Letter

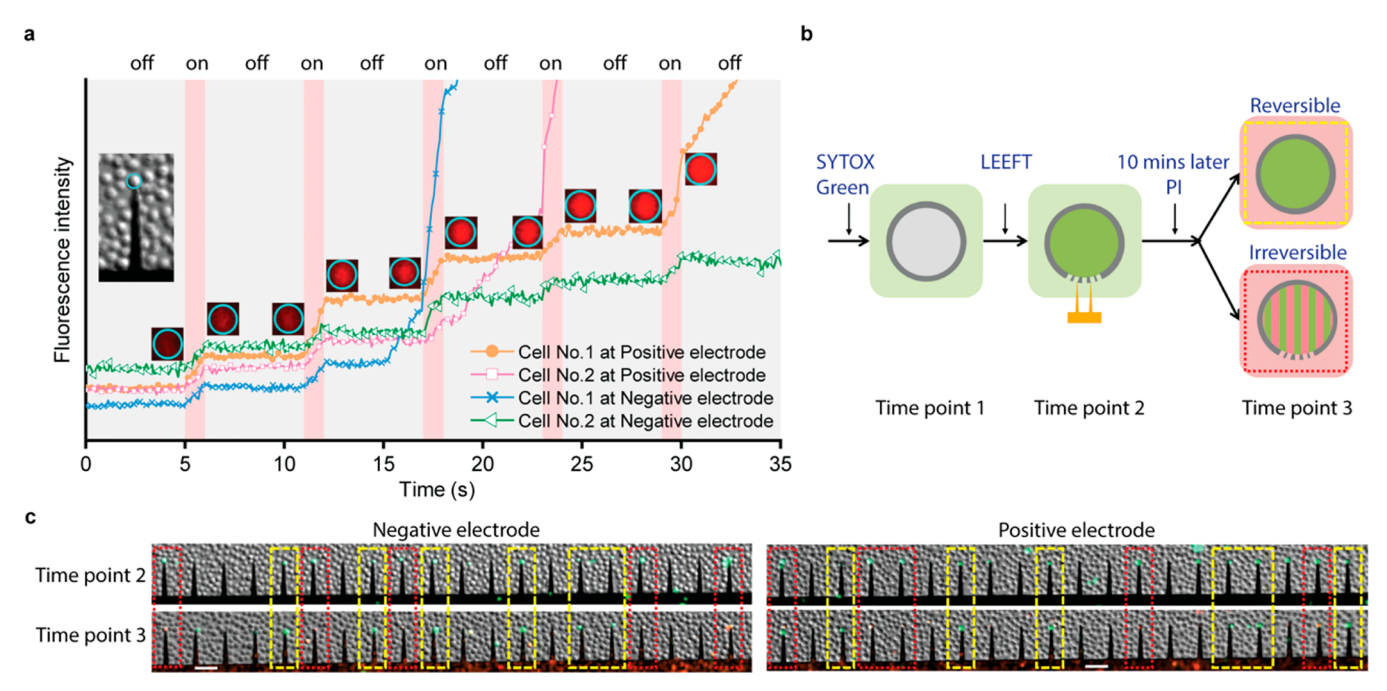


Figure 4. Detection of reversible electroporation. (a) Increase of PI stain fluorescence of four cells at nanowedge tips on positive and negative electrodes, respectively, under intermittent treatment. The red area indicates that the treatment is on, which are $14 \text{ V}/2 \mu\text{s}/100 \mu\text{s}/10 000$ pulses for 1 s total time. The gray area indicates that the treatment is off, which is 0 V for 5 s. The inserted images show Cell No. 1 at the positive electrode (the orange data line). (b) Schematic of the double staining method with SYTOX Green and PI for reversible electroporation detection. (c) Microscopy images showing reversible electroporation under 14 V. The cells inside the yellow frames had reversible pores on membrane since they are stained with SYTOX Green at Time point 2 but are not stained with PI at Time point 3. The cells inside the red frames have irreversible pores since they are first stained with SYTOX Green and then stained with PI. The scale bars are 5 μ m.

gaps (25, 50, 100 μ m) were tested for bacteria inactivation. Under the same applied voltage, the strength of the nanoenhanced electric field will be reversely proportional to the gap between the two electrodes (Figure S6a-c). Therefore, the chips with a smaller gap achieved a higher bacteria inactivation (Figure 3a and Figure S6d). The chips with nanowedges of different intervals (0.8 μ m, 4 μ m, 40 μ m) were also tested. Similarly, because of the stronger lightning-rod effect for electric-field enhancement (Figure S7a,b), the nanowedges with a larger interval in between could achieve higher bacteria inactivation under the same applied voltage (Figure 3b and Figure S7c). When all the results are analyzed together, the percentage of bacteria inactivation at the tips of nanowedges shows a positive correlation with the electric field strength (Figure 3c left), but not with the applied voltages (Figure 3c right). This result indicates that the bacteria inactivation is attributed to the nanoenhanced electric field.

We also found that the bacteria inactivation is not due to reactive oxygen species (ROS). Although inducing ROS is a commonly used antimicrobial method, it has some side effects, such as generating byproducts. Electric field treatment systems could generate ROS especially under high voltages or long treatment times. To test if the bacteria are inactivated by ROS, DCFH-DA stain was used to detect ROS generation. 32,33 In the experimental group with $30 \text{ V}/2 \mu\text{s}/100 \mu\text{s}/100 000$ pulses treatment, DCFH-DA stained cells show no fluorescence (Figure 3d top), suggesting no ROS generation. Meanwhile, >90% bacteria inactivation is achieved (Figure 3d bottom and experimental group, no DMSO in Figure 3h), indicating that this bacteria inactivation is not due to ROS damage. To confirm this ROS detection method is valid, we intentionally induced ROS generation with a much longer pulse width in the

positive control (20 V/200 μ s/10 ms/1000 pulses). The significant green fluorescence of DCFH-DA stained cells shows that ROS is generated near the positive electrode (Figure 3e top). The positive electrode shows more inactivated bacteria at each nanowedge tip than the negative electrode and the experimental group (Figure 3e bottom and positive control, no DMSO in Figure 3h), which could be attributed to the ROS damage.

To further confirm that the bacteria inactivation at 30 V/2 μ s/100 μ s is not due to ROS, a ROS scavenger, DMSO, was added to the medium at 15% (w/w) to quench ROS and protect bacteria from its damage.³⁴ In the positive control group, the bacteria at the positive electrodes are largely protected by DMSO (Figure 3g and positive control in Figure 3h), proving that 15% DMSO is able to protect bacteria from ROS damage. In the experimental group, even with the ROS scavenger, the bacteria inactivation percentage and inactivated cell number are not affected (Figure 3f and experimental group in Figure 3h), which further confirms that the bacteria inactivation at the nanowedge tips is not due to ROS damage.

The third piece of evidence is the quick cell membrane recovery after LEEFT, which supports that electroporation is the main bacteria inactivation mechanism. Reversible electroporation is a phenomenon that pores formed on the lipid bilayer membrane reseal automatically after the electric field is removed. It occurs when the cell is exposed to a relatively weaker electric field or a shorter treatment time. ¹⁴ The changing of PI fluorescence intensity of four cells located at nanowedge tips under 14 V/2 μ s/100 μ s intermittent treatment shows that when the treatment is on (red area, 10 000 pulses for 1 s total time), the fluorescence increases, which means pore formation and PI dye inflow (Figure 4a).

Nano Letters pubs.acs.org/NanoLett Letter

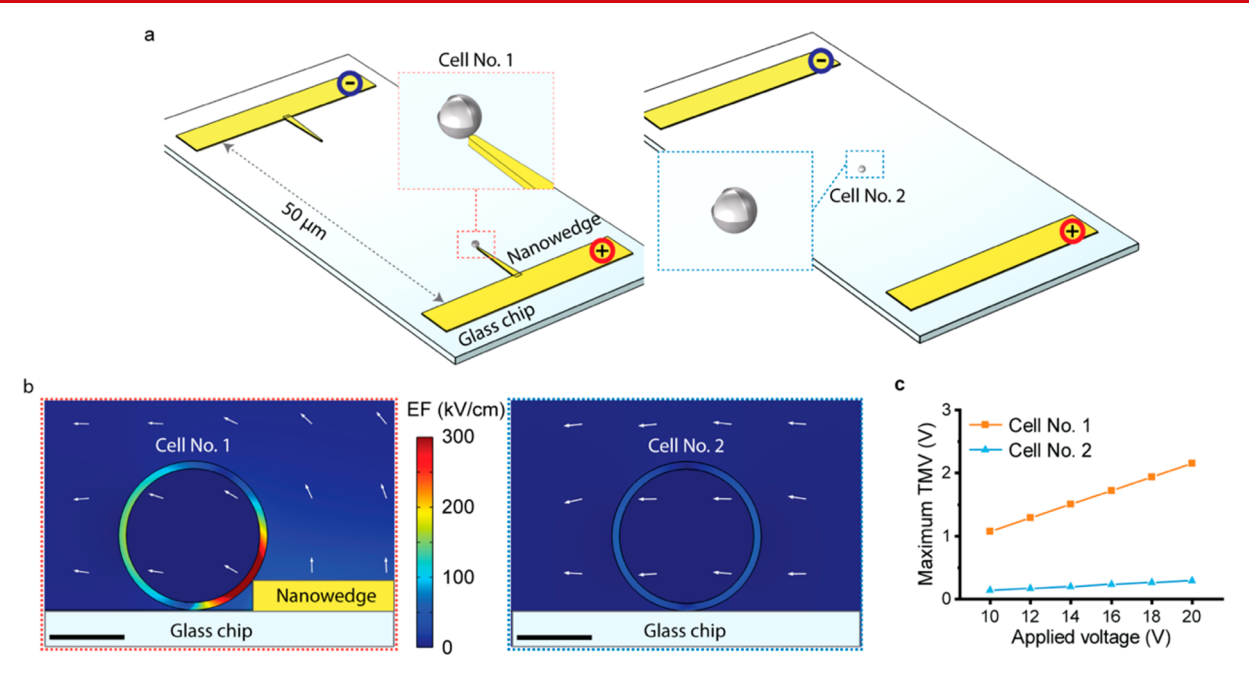


Figure 5. Theoretical analysis of cell TMV in LEEFT and bulk EFT. (a) Simulation set up for LEEFT (left) and bulk EFT (right). (b) Left view of the middle cutting plane showing the electric field across the cell membrane of Cell No. 1 in LEEFT (left) and Cell No. 2 in bulk EFT (right) under 20 V applied voltage. The arrows indicate the direction of the electric field. The scale bars are 0.5 μ m. (c) Maximum TMV on Cell No. 1 and Cell No. 2 under different applied voltages.

When the treatment is removed (gray area, 5 s), the fluorescence stops rising immediately, suggesting that the pores close and the membrane regains its integrity after the treatment stops (Figure 4a). This kind of quick cell membrane recovery is a common phenomenon in reversible electroporation, ^{13,14} but is hard to find in other kinds of membrane damages, such as direct oxidation. Therefore, quick pore reseal is a strong evidence for reversible electroporation.

Reversible electroporation was also detected using a double staining method with SYTOX Green and PI, which are both DNA stains and can only enter cells with compromised membrane.³⁵ SYTOX Green is first added to the medium (Time point 1, Figure 4b). After the treatment is applied, perforated cells are stained with SYTOX Green and show green fluorescence (Time point 2, Figure 4b). After 10 min, PI is added, which could only stain the cells that still have compromised membrane. Thus, the cells that are not stained with PI are considered as having reversible pores (Time point 3, Figure 4b). With a relatively low applied voltage at 14 V (2 μ s/100 μ s/20 000 pulses), some already perforated cells could not then be stained with PI, indicating that the pores formed on the cell membrane are reversible (Figure 4c). While under a high applied voltage at 80 V (1 μ s/1 ms/10 pulses), almost all cell perforation is irreversible (Figure S8). This phenomenon conforms to the feature of electroporation, indicating that electroporation is the predominant mechanism for bacteria inactivation in LEEFT. Note that when 1 s effective treatment time (500 000 pulses) is used, there is no significant reversible damage as shown in Figure 2b. It is mainly due to the longer treatment time, which increases the cell death possibility. It is also possible that although reversible pores close after LEEFT, the long pore open time already allows severe compound transfer between the inside and outside of the cell, which leads to cell function damage and cell inactivation ultimately.

Because of the lightning-rod effect, the electric field at tips of metal rods with a high aspect ratio will be greatly enhanced. Therefore, this strong electric field could be sufficient to charge cell membrane, cause irreversible electroporation, and kill bacteria with lower applied voltages. Although bench-scale LEEFT for water disinfection was developed based on this concept, the mechanism was only supported by control experiments done with electrodes with/without nanowire modifications. 19,20 There was no direct evidence confirming that the bacteria were inactivated due to the locally enhanced electric field and electroporation. The results achieved in this study provide important evidence on the mechanism. First, only the bacteria located in the locally enhanced electric field are inactivated while others in bulk are intact (Figure 1b,d). The inactivation percentage shows a positive correlation with the strength of the locally enhanced electric field instead of the applied voltage (Figure 3c). Furthermore, when >90% bacteria inactivation is achieved with LEEFT at 30 V/2 μ s/100 μ s, there is no significant ROS generation (Figure 3d), indicating this bacteria inactivation is not due to ROS damage. Reversible electroporation is detected under relatively lower applied voltage (Figure 4), suggesting that LEEFT could induce electroporation, and irreversible electroporation causing bacteria inactivation could be dominant at higher voltages.

It is worth noticing that the electric field enhancement by nanowedges is the same for both positive and negative electrodes theoretically (Figures S6 and S7). Consistently, all of the bacteria inactivation phenomena discussed above do not show a significant difference between the positive and negative electrodes. An electrochemical disinfection study reported that anode induced significantly higher bacteria inactivation than cathode, suggesting that electrical reduction should not cause the same level of cell damage as electrical oxidation. Our positive control group for ROS detection also confirms this (Figure 3e). Therefore, the same phenomenon on both electrodes found in this work indicates that electrical oxidation/reduction should not be the mechanism causing bacteria inactivation. Also, metal ions should not play a role in

Nano Letters pubs.acs.org/NanoLett Letter

bacteria inactivation either. Since gold is electrochemically stable, under the very short 2 μ s pulses at voltages lower than 30 V, there should be no significant gold ion release. Therefore, electroporation is demonstrated as the predominant mechanism causing bacteria inactivation in LEEFT.

Since electroporation is the predominant mechanism, the induced transmembrane voltage (TMV), which is the increased potential difference across the cell membrane resulting from the exposure to an external electric field, was analyzed theoretically using finite element simulation to compare LEEFT and bulk EFT. Both the on-chip system like the one used in this work (Figure 5) and a 3D system with a standing nanowire (Figure S9) were simulated. One cell in LEEFT and one cell in bulk EFT are compared, which is Cell No. 1 located at the nanowedge tip (Figure 5a left), and Cell No. 2 located between two electrodes without nanowedge (Figure 5a right). The simulation results show that the voltage drop across the membrane, that is, the electric field, is greatly enhanced at Cell No. 1 near the nanowedge tip (Figure 5b left) compared to Cell No. 2 (Figure 5b right). The maximum TMVs of the two cells show that with the same applied voltage, Cell No. 1 in LEEFT located at the nanowire tip can achieve around 7.5 times higher TMV than Cell No. 2 in bulk EFT (Figure 5c), indicating that much lower voltage could be applied to achieve the same level of TMV on cells in LEEFT than in bulk EFT.

This work is a single-cell level proof-of-concept study of LEEFT. We are optimistic that LEEFT can have plenty of applications. The bacteria inactivation at nanowedge tips does not require ROS generation, which minimizes the side reactions, making it suitable for high-quality sample processing, such as liquid food or blood sample. LEEFT effectively kills bacteria with lower voltages and short pulses, which makes it safe for medical applications, such as wound healing, and energy-efficient for large-scale treatment processes, such as water treatment. Since the bacteria inactivation is highly localized, it is perfect for surface treatment, such as biofilm and biofouling prevention. Furthermore, it can also find applications in continuous flow systems since bacteria could be attracted to the nanowedge tips and become inactivated. The as-shown rapid cell damage and the effectiveness of both electrodes further improve its efficiency. Since electroporation targets the phospholipid membrane, LEEFT should work on a broad range of cell types with more applications, including intracellular molecule delivery and cell lysing.³⁷

In real applications, the efficiency of LEEFT could be improved through several ways. Electrodes all covered with nanowires could be developed to increase the effective zones. The treatment system design and operation processes could be improved depending on different applications. For instance, fluid mixing can be introduced in continuous flow systems to improve the possibility of transporting bacteria to the nanowire tips. The pulse width and voltage of the electrical pulses could be altered to effectively manipulate cells in the flow, such as to attract bacteria cells to the nanowire tips or to repulse the dead cells away from the tips. For large scale applications, the cost could be reduced by using cheaper electrode materials, such as Cu electrodes with CuO or Cu₃P nanowires synthesized on the surface. The synergistic effect of electroporation with metal ions, 38,39 ozone, 25 and other antimicrobial reagents could also be applied to further improve the efficiency of LEEFT.

ASSOCIATED CONTENT

Supporting Information

The Supporting Information is available free of charge at https://pubs.acs.org/doi/10.1021/acs.nanolett.1c02240.

Materials and methods; Figures S1–S9 showing the digital photo of the lab-on-a-chip, experimental setup, waveform, electrodes having no nanowedges as a control, cell decay after LEEFT, chips of different electrode gap, chips with nanowedges of different intervals, irreversible electroporation at 80 V, simulation of TMV; screen shots of Movie S1–S4 and the captions (PDF)

Movie S1: Bacteria inactivation process in LEEFT (MP4)

Movie S2: Transport and inactivation of free-moving S. epidermidis cells in LEEFT (MP4)

Movie S3: Transport and inactivation of free-moving *E. coli* cells in LEEFT (MP4)

Movie S4: Transport and inactivation of free-moving *B. subtilis* cells in LEEFT (MP4)

AUTHOR INFORMATION

Corresponding Author

Xing Xie — School of Civil and Environmental Engineering and Institute for Electronics and Nanotechnology, Georgia Institute of Technology, Atlanta, Georgia 30332, United States; orcid.org/0000-0002-2253-0964; Email: xing.xie@ce.gatech.edu

Authors

Ting Wang — School of Civil and Environmental Engineering, Georgia Institute of Technology, Atlanta, Georgia 30332, United States; orcid.org/0000-0002-4658-7789

Devin K. Brown – Institute for Electronics and Nanotechnology, Georgia Institute of Technology, Atlanta, Georgia 30332, United States

Complete contact information is available at: https://pubs.acs.org/10.1021/acs.nanolett.1c02240

Author Contributions

X.X. and T.W. designed the research. T.W. performed the research. D.K.B. contributed new reagents/analytic tools. T.W. and X.X. analyzed the data and wrote the paper.

Notes

The authors declare no competing financial interest.

ACKNOWLEDGMENTS

The authors acknowledge the financial support from the National Science Foundation [Grant number CBET 1845354]. This work was performed in part at the Georgia Tech Institute for Electronics and Nanotechnology, a member of the National Nanotechnology Coordinated Infrastructure (NNCI), which is supported by the National Science Foundation [Grant Number ECCS-1542174]. T.W. is grateful for the financial support provided by the China Scholarship Council.

■ REFERENCES

- (1) Neu, H. C. The crisis in antibiotic resistance. *Science* **1992**, 257 (5073), 1064–1073.
- (2) Sedlak, D. L.; von Gunten, U. The chlorine dilemma. *Science* **2011**, 331 (6013), 42–43.

- (3) McKinney, C. W.; Pruden, A. Ultraviolet disinfection of antibiotic resistant bacteria and their antibiotic resistance genes in water and wastewater. *Environ. Sci. Technol.* **2012**, *46* (24), 13393–13400.
- (4) Hijnen, W. A. M.; Beerendonk, E. F.; Medema, G. J. Inactivation credit of UV radiation for viruses, bacteria and protozoan (oo)cysts in water: A review. *Water Res.* **2006**, *40* (1), 3–22.
- (5) Gao, S.; Hemar, Y.; Ashokkumar, M.; Paturel, S.; Lewis, G. D. Inactivation of bacteria and yeast using high-frequency ultrasound treatment. *Water Res.* **2014**, *60*, 93–104.
- (6) Lu, H.; Mutafopulos, K.; Heyman, J. A.; Spink, P.; Shen, L.; Wang, C.; Franke, T.; Weitz, D. A. Rapid additive-free bacteria lysis using traveling surface acoustic waves in microfluidic channels. *Lab Chip* **2019**, *19* (24), 4064–4070.
- (7) Plazas-Tuttle, J.; Das, D.; Sabaraya, I. V.; Saleh, N. B. Harnessing the power of microwaves for inactivating Pseudomonas aeruginosa with nanohybrids. *Environ. Sci.: Nano* **2018**, *5* (1), 72–82.
- (8) Grahl, T.; Markl, H. Killing of microorganisms by pulsed electric fields. *Appl. Microbiol. Biotechnol.* **1996**, 45 (1–2), 148–157.
- (9) Barba, F. J.; Parniakov, O.; Pereira, S. A.; Wiktor, A.; Grimi, N.; Boussetta, N.; Saraiva, J. A.; Raso, J.; Martin-Belloso, O.; Witrowa-Rajchert, D.; Lebovka, N.; Vorobiev, E. Current applications and new opportunities for the use of pulsed electric fields in food science and industry. *Food Res. Int.* **2015**, *77*, 773–798.
- (10) Kotnik, T.; Frey, W.; Sack, M.; Meglič, S. H.; Peterka, M.; Miklavčič, D. Electroporation-based applications in biotechnology. *Trends Biotechnol.* **2015**, 33 (8), 480–488.
- (11) Bendicho, S. I.; Barbosa-Cánovas, G. V.; Martín, O. Milk processing by high intensity pulsed electric fields. *Trends Food Sci. Technol.* **2002**, 13 (6–7), 195–204.
- (12) Gusbeth, C.; Frey, W.; Volkmann, H.; Schwartz, T.; Bluhm, H. Pulsed electric field treatment for bacteria reduction and its impact on hospital wastewater. *Chemosphere* **2009**, *75* (2), 228–233.
- (13) Sengel, J. T.; Wallace, M. I. Imaging the dynamics of individual electropores. *Proc. Natl. Acad. Sci. U. S. A.* **2016**, 113 (19), 5281–5286
- (14) Kotnik, T.; Rems, L.; Tarek, M.; Miklavčič, D. Membrane electroporation and electropermeabilization: mechanisms and models. *Annu. Rev. Biophys.* **2019**, *48*, 63–91.
- (15) Tieleman, D. P.; Leontiadou, H.; Mark, A. E.; Marrink, S.-J. Simulation of pore formation in lipid bilayers by mechanical stress and electric fields. *J. Am. Chem. Soc.* **2003**, *125* (21), 6382–6383.
- (16) Wang, T.; Chen, H.; Yu, C.; Xie, X. Rapid determination of the electroporation threshold for bacteria inactivation using a lab-on-a-chip platform. *Environ. Int.* **2019**, *132*, 105040.
- (17) Yildiz, S.; Pokhrel, P. R.; Unluturk, S.; Barbosa-Canovas, G. V. Shelf life extension of strawberry juice by equivalent ultrasound, high pressure, and pulsed electric fields processes. *Food Res. Int.* **2021**, *140*, 110040.
- (18) Rojas-Chapana, J. A.; Correa-Duarte, M. A.; Ren, Z.; Kempa, K.; Giersig, M. Enhanced introduction of gold nanoparticles into vital acidothiobacillus ferrooxidans by carbon nanotube-based microwave electroporation. *Nano Lett.* **2004**, *4* (5), 985–988.
- (19) Liu, C.; Xie, X.; Zhao, W.; Liu, N.; Maraccini, P. A.; Sassoubre, L. M.; Boehm, A. B.; Cui, Y. Conducting nanosponge electroporation for affordable and high-efficiency disinfection of bacteria and viruses in water. *Nano Lett.* **2013**, *13* (9), 4288–4293.
- (20) Huo, Z.-Y.; Xie, X.; Yu, T.; Lu, Y.; Feng, C.; Hu, H.-Y. Nanowire-modified three-dimensional electrode enabling low-voltage electroporation for water disinfection. *Environ. Sci. Technol.* **2016**, *S0* (14), 7641–7649.
- (21) Huo, Z.-Y.; Zhou, J.-F.; Wu, Y.; Wu, Y.-H.; Liu, H.; Liu, N.; Hu, H.-Y.; Xie, X. A Cu 3 P nanowire enabling high-efficiency, reliable, and energy-efficient low-voltage electroporation-inactivation of pathogens in water. *J. Mater. Chem. A* **2018**, *6* (39), 18813–18820.
- (22) Huo, Z.-Y.; Liu, H.; Wang, W.-L.; Wang, Y.-H.; Wu, Y.-H.; Xie, X.; Hu, H.-Y. Low-voltage alternating current powered polydopamine-protected copper phosphide nanowire for electroporation-disinfection in water. *J. Mater. Chem. A* **2019**, *7* (13), 7347–7354.

- (23) Huo, Z.-Y.; Kim, Y.-J.; Suh, I.-Y.; Lee, D.-M.; Lee, J. H.; Du, Y.; Wang, S.; Yoon, H.-J.; Kim, S.-W. Triboelectrification induced self-powered microbial disinfection using nanowire-enhanced localized electric field. *Nat. Commun.* **2021**, *12* (1), 1–11.
- (24) Huo, Z.-Y.; Liu, H.; Yu, C.; Wu, Y.-H.; Hu, H.-Y.; Xie, X. Elevating the stability of nanowire electrodes by thin polydopamine coating for low-voltage electroporation-disinfection of pathogens in water. *Chem. Eng. J.* **2019**, *369*, 1005–1013.
- (25) Zhou, J.; Wang, T.; Xie, X. Locally Enhanced Electric Field Treatment (LEEFT) Promotes the Performance of Ozonation for Bacteria Inactivation by Disrupting the Cell Membrane. *Environ. Sci. Technol.* **2020**, *54* (21), 14017–14025.
- (26) Zhou, J.; Wang, T.; Chen, W.; Lin, B.; Xie, X. Emerging investigator series: locally enhanced electric field treatment (LEEFT) with nanowire-modified electrodes for water disinfection in pipes. *Environ. Sci.: Nano* **2020**, *7* (2), 397–403.
- (27) Zhou, J.; Wang, T.; Yu, C.; Xie, X. Locally enhanced electric field treatment (LEEFT) for water disinfection. *Front. Environ. Sci. Eng.* **2020**, *14*, 1–12.
- (28) Zhou, J.; Yu, C.; Wang, T.; Xie, X. Development of nanowire-modified electrodes applied in the locally enhanced electric field treatment (LEEFT) for water disinfection. *J. Mater. Chem. A* **2020**, 8 (25), 12262–12277.
- (29) Jiang, X.; Hu, J.; Petersen, E. R.; Fitzgerald, L. A.; Jackan, C. S.; Lieber, A. M.; Ringeisen, B. R.; Lieber, C. M.; Biffinger, J. C. Probing single-to multi-cell level charge transport in Geobacter sulfurreducens DL-1. *Nat. Commun.* **2013**, *4* (1), 1–6.
- (30) Wang, T.; Yu, C.; Xie, X. Microfluidics for Environmental Applications; Springer Berlin: Berlin, 2020; pp 1-24.
- (31) Lapizco-Encinas, B. H.; Simmons, B. A.; Cummings, E. B.; Fintschenko, Y. Dielectrophoretic concentration and separation of live and dead bacteria in an array of insulators. *Anal. Chem.* **2004**, *76* (6), 1571–1579.
- (32) Zhang, T.; Wang, T.; Mejia-Tickner, B.; Kissel, J.; Xie, X.; Huang, C.-H. Inactivation of Bacteria by Peracetic Acid Combined with Ultraviolet Irradiation: Mechanism and Optimization. *Environ. Sci. Technol.* **2020**, *54* (15), 9652–9661.
- (33) Huang, X.; Chen, X.; Chen, Q.; Yu, Q.; Sun, D.; Liu, J. Investigation of functional selenium nanoparticles as potent antimicrobial agents against superbugs. *Acta Biomater.* **2016**, 30, 397–407.
- (34) Guo, Y.; Cheng, C.; Wang, J.; Wang, Z.; Jin, X.; Li, K.; Kang, P.; Gao, J. Detection of reactive oxygen species (ROS) generated by TiO2 (R), TiO2 (R/A) and TiO2 (A) under ultrasonic and solar light irradiation and application in degradation of organic dyes. *J. Hazard. Mater.* **2011**, 192 (2), 786–793.
- (35) Vaessen, E.; Timmermans, R.; Tempelaars, M.; Schutyser, M.; den Besten, H. Reversibility of membrane permeabilization upon pulsed electric field treatment in lactobacillus plantarum WCFS1. *Sci. Rep.* **2019**, *9* (1), 1–11.
- (36) Liu, H.; Ni, X.-Y.; Huo, Z.-Y.; Peng, L.; Li, G.-Q.; Wang, C.; Wu, Y.-H.; Hu, H.-Y. Carbon fiber-based flow-through electrode system (FES) for water disinfection via direct oxidation mechanism with a sequential reduction—oxidation process. *Environ. Sci. Technol.* **2019**, 53 (6), 3238–3249.
- (37) Liu, P.; Zhou, J.; Wang, T.; Yu, C.; Hong, Y.; Xie, X. Efficient microalgae inactivation and growth control by locally enhanced electric field treatment (LEEFT). *Environ. Sci.: Nano* **2020**, *7* (7), 2021–2031.
- (38) Zhou, J.; Wang, T.; Xie, X. Rationally designed tubular coaxial-electrode copper ionization cells (CECICs) harnessing non-uniform electric field for efficient water disinfection. *Environ. Int.* **2019**, *128*, 30–36.
- (39) Chen, W.; Jiang, J.; Zhang, W.; Wang, T.; Zhou, J.; Huang, C.-H.; Xie, X. Silver nanowire-modified filter with controllable silver ion release for point-of-use disinfection. *Environ. Sci. Technol.* **2019**, 53 (13), 7504–7512.